2.8 The generalized transmission-line model

The guitar is part of a signal-processing system generating sound from the movement of a plectrum (pick). With the input quantities of plectrum-force and plectrum-velocity, and the output quantities of bearing force and bearing velocity (in an acoustic guitar), or pickup voltage and pickup current (in the electric guitar), respectively, the string is a subsystem of the guitar. In Chapter 1.5 we had defined the plucking process as imprinting a force step with the effect that a special square wave runs back and forth on the string. This (more of less) periodic repetition of the excitation signal may be very nicely described with signal-flow diagrams, as they are also used in the context of digital FIR-/IIR-filters. It is not a problem that the signals in digital filters are usually time-discrete and discrete-valued, while the signals on the string are time- and value-continuous. In the simple transmission-line model, only the delay times occurring between the string bearings are emulated via delay lines. Conversely, plucking point and pickup position may be arbitrarily chosen.

2.8.1 Ideal string, bridge pickup

The following signal flow diagrams **SFD** (block diagrams) represent the signal processing via arithmetical operations. The basic operations are delay, summation, subtraction, and multiplication with a constant. The graphs do not give any indication of the source- and load-impedances and must not be confused with a circuit diagram.

A transverse force jumping to zero at the time $t = 0$ is defined as the excitation signal for the string. This force step runs in both directions from the plucking point; its phase velocity is c. The delay time necessary to reach bridge or nut, respectively, depends on c and the distance that needs to be covered. At the end of the string, each force step is reflected – here, we need to distinguish between $r_{bridge} = R$ and $r_{nut} = r$. Thereafter, both force steps circle in a recursive loop with an overall delay time of $T = 2L/c$. **Fig. 2.26** shows the corresponding SFD:

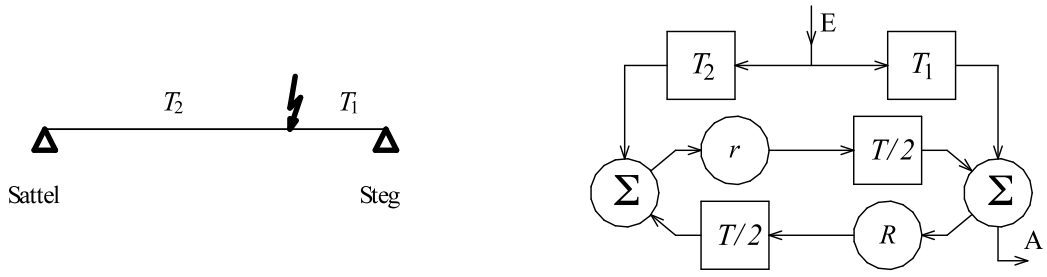

Fig. 2.26: Signal flow diagram (SFD) for non-dispersive string vibration. T_1 and T_2 are delay times from the plucking point to the bridge ("Steg") and the nut ("Sattel"), respectively; R is the reflection coefficient at the bridge, r is the reflection coefficient at the nut, $T/2$ is the delay time between bridge and nut, or nut and bridge, respectively. E = input, A = output (bridge).

The SFD shown in Fig. 2.26 differs from the ideal string in one significant aspect: the impulse created by the plucking runs back and forth on one and the same string, while in the SFD, the paths in the two directions manifest themselves in two separate, serially connected signal branches. Still, the signal processing is identical, and in both cases one cycle includes *two* reflections.

By repositioning of single delays, the SFD can be reshaped to result in a ladder network of three systems (**Fig. 2.27**):

- A basic delay T_1, modeling the delay time from point of plucking to the bridge.
- A recursive system with the delay time T, modeling the string vibration maintained via the reflections (IIR- and AR-filter respectively)
- Am interference filter with a delay difference of $2T_2$, modeling the shaping of the sound color via the point of plucking (FIR- and MA-Filter, respectively). For any one reflection at the nut /(or fret), $r \approx -1$ holds.

This representation has the main advantage that the "plucking"-filter (FIR-filter) and the section of the generator (IIR-filter) are considered independently from each other in separate stages. Assuming un-damped, loss-free vibrations ($R \cdot r = 1$), the IIR-filter (operating just shy of self-oscillation) generates – after impulse excitation – a periodic signal. Obligatorily, there is a matching harmonic line spectrum with the frequency distance of the lines equal to the fundamental frequency of the string.

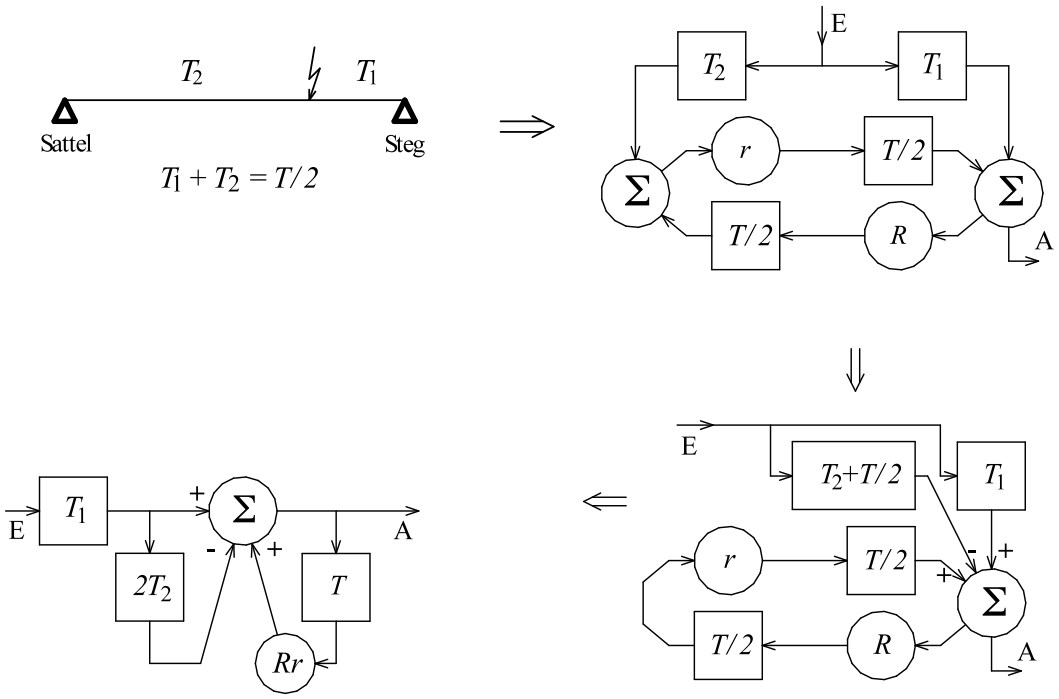

Fig. 2.27: Rearranged signal flow diagram (only a single signal path string → bridge). The sequence of the FIR-filter ($2T_2$) and the IIR-filter (T) is permutable (commutative mapping in the linear system). "Sattel" = nut, "Steg" = bridge.

Rearranging the FIR-delay time is done with $T_1 + T_2 = T/2$, resulting in:

$$(T_2 + T/2) - T_1 = T_2 + T/2 - (T/2 - T_2) = 2T_2$$

Using simple methods known from signal processing [e.g. 5], we can now derive from the SFD shown in Fig. 2.27 the behavior regarding frequency. If we take, as excitation signal, a short impulse (idealized a Dirac) periodically repeated in the IIR-filter, a spectrum with equidistant lines of constant height results. This spectrum is filtered as it runs through the subsequent systems, i.e. it is modified.

A pure signal delay by a constant delay time (e.g. T_1) only changes the phase spectrum but not the magnitude spectrum. We will ignore this basic delay since it is immaterial for the following considerations whether or not the output signal arrives a few milliseconds later. However, the delay time in the FIR-filter must not be ignored since here two signals are superimposed that are delayed with respect to each other – with the resulting frequency-selective amplifications and cancellations (comb-filter). The sequence of FIR/IIR, or IIR/FIR, respectively, must not be interchanged.

The filter effect of the **comb-filter** is extensively described in literature; we will only cover it in short here. The temporal input signal of a delay line arrives at the output after a delay (generally: T_x), the spectrum of the input signal is to be multiplied with the transfer function to yield the spectrum of the output signal. The transfer function $\underline{H}$ of a (pure) delay line with the delay T_x is:

$$\underline{H}(j\omega) = e^{-j\omega T_x}; \qquad \omega = 2\pi f \qquad \text{Transfer function of a delay line}$$

In a comb-filter, delayed signal and un-delayed signal are added or subtracted, respectively; this yields the transfer function of the comb-filter:

$$\underline{H}_{FIR} = 1 - \exp(-j\omega T_x); \qquad \left|\underline{H}_{FIR}\right| = 2 \cdot \left|\sin(\omega T_x / 2)\right| \qquad \text{FIR-filter}$$

The designation **FIR-filter** (Finite Impulse Response) is due the impulse response being of finite duration. The magnitude of the frequency response is the magnitude of a sine-function with zeroes at 0 Hz and integer multiples of the reciprocal of the delay time T_x. This calculation is formally correct but inconvenient for illustrations, as **Fig. 2.28** shows. Similar problems are known from time-discrete signals if the sampling theorem is not adhered to: too low a sampling rate results in (usually undesirable) reverse convolution. In the present special case, however, the ambiguity due to the sampling is helping. Via the identity

$$\left|\sin(m\pi - \varphi)\right| \equiv \left|\sin(\varphi)\right| \text{ only for } m = \text{integer}$$

and a few intermediate steps, the FIR-transfer function may be converted into:

$$\left|\underline{H}_{FIR}\right| = \left|\sin\left(\pi \cdot \frac{f}{f_G} \cdot \frac{d}{M}\right)\right| \qquad \text{FIR-filter, reformulated}$$

Herein, d represents the distance between the plucking point and the bridge, and M is the length of the open string (scale). For the fretted string, the scale needs to be applied here, as well, because it is included in the formula for the propagation speed of the wave. If the open string is plucked precisely in the middle, the long-term spectrum holds only odd harmonics – the zeroes of the sine-function are located at the even harmonics. The closer the plucking point is to the bridge, the wider the minima of the envelope are spaced. The conversion only holds in the steady-state part (discrete line-spectrum) but not for the transitory process. This is a basic condition for every transfer function, though: it always holds for the steady state only. Furthermore, we need to consider that the delays in the above model are frequency-independent – dispersion is not (yet) emulated. Spread-out spectra require, instead of simple delay lines, **all-passes** that approximate the string dispersion in the frequency response of their delay (Chapter 2.8.4).

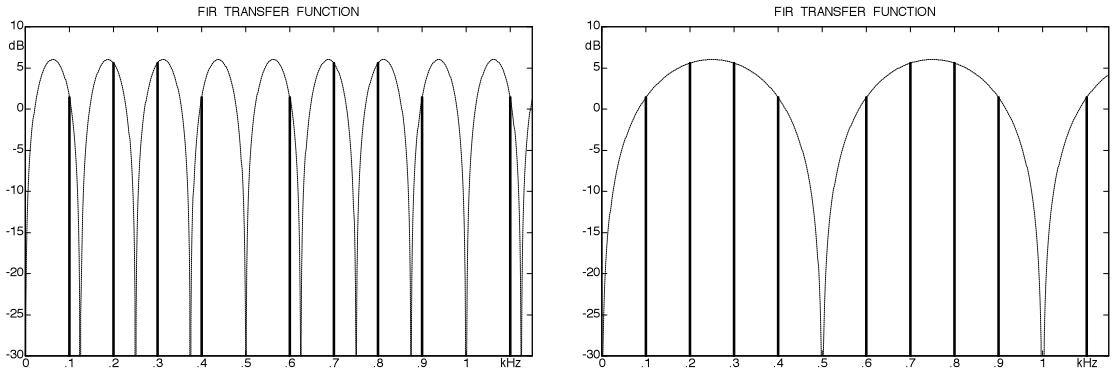

Fig. 2.28: FIR-filter frequency response (magnitude, ---) and filtered line spectrum for $d = M/5$. The lines shown are identical in both graphs; the graph on the right shows the transformed FIR-transfer-function.

In **Fig. 2.29** we see the measurements for a plucked E_2-string. The distance between plucking location and bridge amounted to d = 4,7 cm and 1,5 cm, respectively. From the results, the first minimum of the comb-filter calculates as 1,1 kHz and 3,5 kHz, respectively. In the low frequency region, the comb-filter structure is clearly visible in the spectral envelope – it is however perturbed by strain-wave resonances (Chapter 1.4, marked via dots). In anticipation of Chapter 2.8.4, Fig. 2.29 already includes the dispersive spreading of the spectral envelope. In addition, further selective damping mechanisms have an effect, especially in the high frequency domain. The associated causes will be elaborated on in Chapter 7.

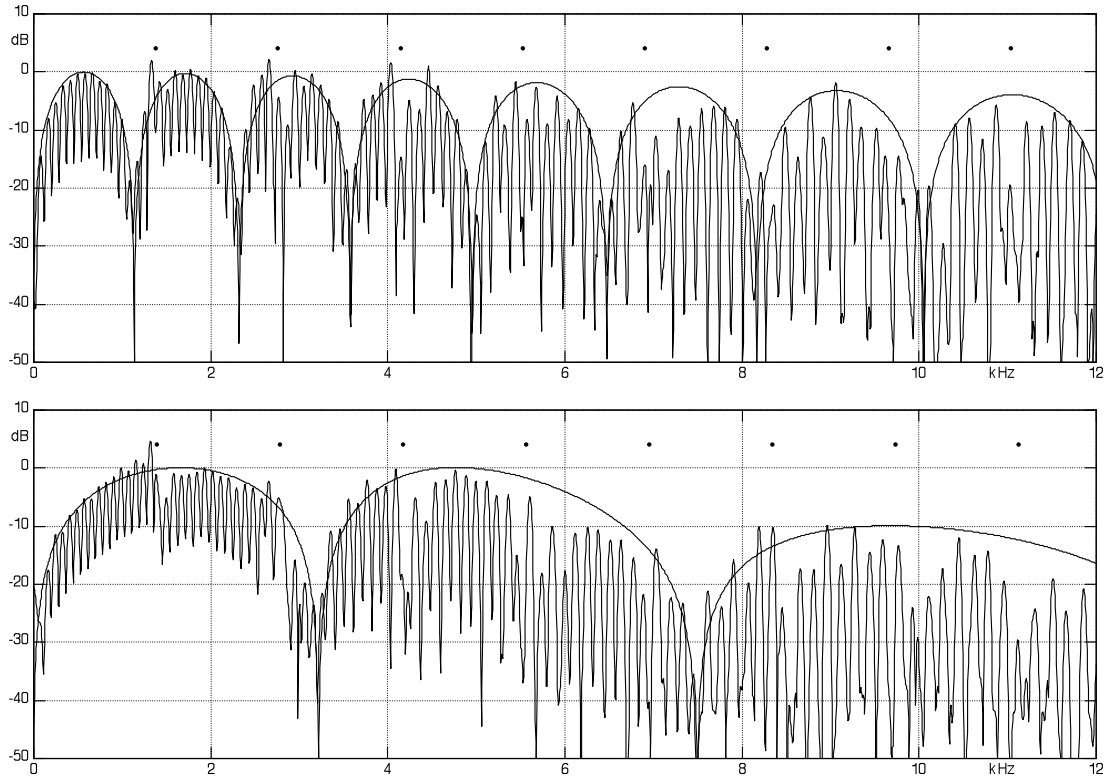

Fig. 2.29: Measured spectra; E_2-string (impulse excitation), d = 4,7 cm (top) and d = 1,5 cm (bottom). The shown envelope was spread out (dispersion) and slightly attenuated towards the high frequencies. The two measurements were taken with two different E_2-strings (OVATION Viper EA-68).

While the FIR-filter determines the spectral envelope, the recursive filter defines the frequency of the individual spectral lines. The impulse response of a recursive filter is of infinite length, which is why the term **IIR-filter** (Infinite Impulse Response) is common for this filter type. With both reflection coefficients being equal to 1, a short excitation impulse would circulate in the loop indefinitely without attenuation; such a filter is called borderline stable. Real strings have reflection coefficients of <1; the impulse-shaped excitation therefore decays over time. For a run through the full loop, both reflection coefficients act in multiplicative manner ($R \cdot r$).

Given $R \cdot r = 0{,}9$, for example, the height of the impulse decreases e.g. from 1 to 0,9 for a single loop, to 0,81 for a double look, and to $0{,}9^n$ for an n-fold loop. The amplitudes of the impulses following each other with a distance in time of T represent a geometric progression; for $R \cdot r < 1$, the term used is **exponential decay**. Chapter 1.6 had already included quantitative statements regarding the decay process; for the guitar string, the loop coefficients are very close to 1 (e.g. 0,993). In the FIR-filter only a single reflection occurs, and therefore $r = -1$ may be used with very good approximation. However, in the IIR-filter, the loop is run through an infinite number of times, and consequently this approximation is not allowable.

Chapter 2.5 had shown that the reflection coefficient is not constant but frequency-dependent. The reason are resonances in the bridge and the nut (or fret) formed from a combination of springs and masses. These springs and masses are not necessarily all found within the bridge (or the nut or fret) but may be located e.g. in the neck of the guitar and act on the nut [8]. When integrating a frequency-dependent reflection coefficient into the SFD (Fig. 2.17), we need to pay attention to the fact that the system shown as circle ($R \cdot r$) becomes a filter that way: $R \cdot r(j\omega)$ is the frequency dependent transfer function of this **reflection filter**. The decay time-constant for each partial results from the loop-delay-time T (frequency dependent if the dispersion is considered), and from $R \cdot r(j\omega)$. The SFD (Fig. 2.27) does not consider the reason for the damping: it is the *overall* damping that is modeled via $R \cdot r(j\omega)$. If required, several individual filters may be connected in series, for example to be able to model the internal string damping in a separate subsystem.

Ahead of the input designated with E in Fig. 2.27 we need to position the **plectrum filter** that shapes the real excitation force from the ideal step (or from an impulse). The **piezo-filter**, or – for acoustic guitars – the body- and radiation-filter follows the output A. The structure-borne sound path is not modeled herein. If we think of the nut merely as a vibration absorber, this is not necessary, either: the damping caused by the nut is considered in $R \cdot r$, after all. However, part of the vibration energy flowing into the nut might be radiated, or fed back to the string via the bridge – something that necessarily would have to work in reverse, as well. The dilatational waves discussed in Chapter 1.4 use a similar bypass (albeit directly via the string).

Additional recursive loops enable a simple emulation of such parallel paths. It should be emphasized again, though, that this does not automatically make for a correct representation of the energy flows. In the SFD, a summation point adds two signals (e.g. two forces), but it does not model the impedances – these would a have to be considered separately depending on the circumstances.

2.8.2 String with single-coil pickup

The SFD presented in Fig. 2.26 is now extended by the output of a magnetic pickup, assuming that the pickup will not influence the vibration of the string. This assumption is not fundamentally justified, because the attraction force of the permanent magnet does change the string vibration, and moreover the law of energy conservation demands that the string delivers the electrical energy generated. While the latter effect may be neglected when high-impedance pickups are deployed, strong magnets are indeed known for their interference when adjusted too close to the strings (Chapter 4.11). However, on order to explain the transfer characteristic in principle, the attraction does not need to be modeled.

Fig. 2.30 depicts the simplified model for the ideal string and a single–coil pickup. T_1 and T_2 designate the delay from the plucking point to the bridge and the nut, respectively. τ_1 and τ_2, respectively, is the delay from the location of the pickup to the bridge and the nut. Multiple rearranging of the drawing yields a ladder network consisting of four different filters:

- A basic delay from plucking point to pickup
- An FIR-filter with the long delay $2T_2$ (or $2\tau_2$, respectively)
- A recursive IIR-filter to model the string vibration
- An FIR-filter with the short delay $2\tau_1$ (or $2T_1$, respectively)

The sequence of these four subsystems may be changed arbitrarily. The pitch depends on the IIR-filter, and the sound color depends on the FIR-filters with their interference effect retraceable to the delay times T_1 and τ_1. There are three cases for the position of the pickup and the plucking point: $T_1 < \tau_1$, $T_1 > \tau_1$, and $T_1 = \tau_1$. It is immaterial whether pickup or plucking point is located closer to the bridge. For example, the pickup may be mounted 10 cm off the bridge, and the string is plucked 4 cm from the bridge, or the pickup may be mounted 4 cm from the bridge and the plucking may happen 10 cm from the bridge – in a *linear model*, the result will be the same (Fig. 2.35). What is not modeled: the string hitting and bouncing off the frets.

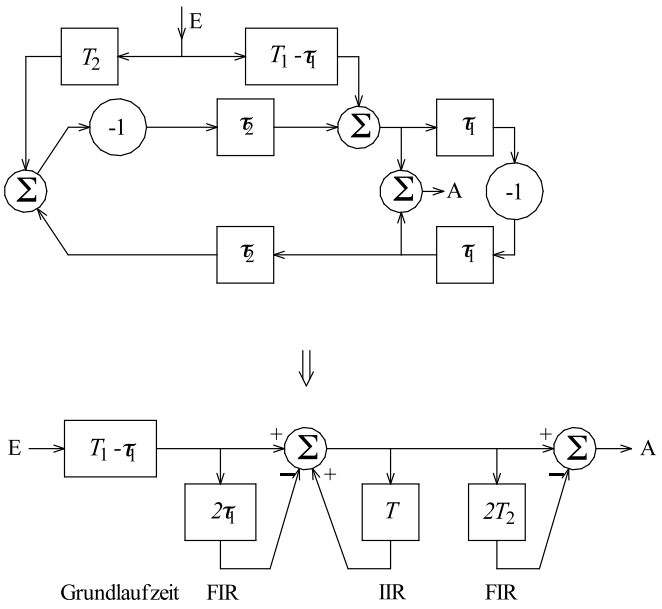

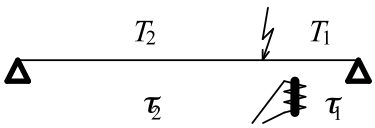

Fig. 2.30a: Ideal string with single-coil magnetic pickup, $T_1 \geq \tau_1$.
Reflections at bridge and nut are taken to be loss-free ($R = r = -1$).
"Grundlaufzeit" = basic delay time

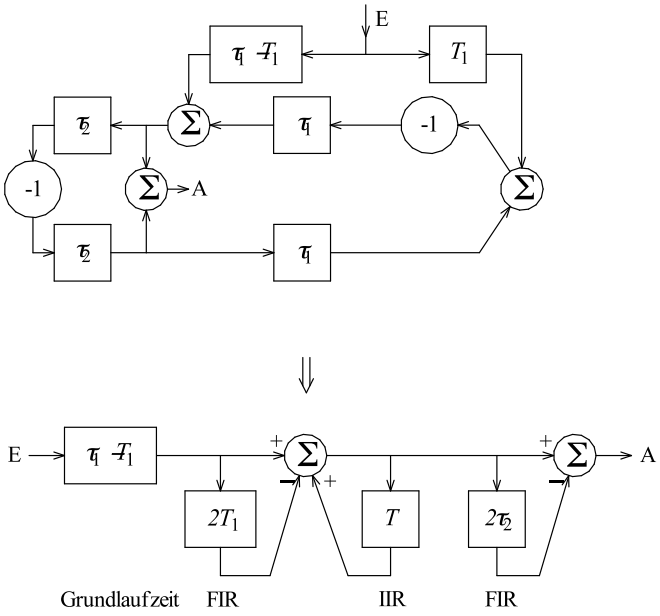

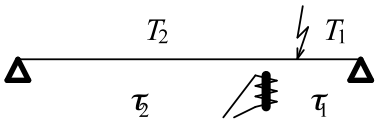

Fig. 2.30b: Ideal string with single-coil magnetic pickup, $T_1 \leq \tau_1$.
Reflections at bridge and nut are taken to be loss-free ($R = r = -1$).
"Grundlaufzeit" = basic delay time

The **step response** associated with the step excitation is indicated in **Fig. 2.31**. Like Fig. 2.30, Fig. 2.31 shows that when changing from $T_1 < \tau_1$ to $T_1 > \tau_1$, merely the delay times T_1 and τ_1 need to be interchanged. The periodicity of this dispersion-free filter is $T = 2(T_1 + T_2) = 2(\tau_1 + \tau_2)$. Two square impulses are located within that period, centered around the point in time t_0, and $T - t_0$, respectively. For $T_1 < \tau_1$ we get $t_0 = \tau_1$, while $t_0 = T_1$ results for $T_1 > \tau_1$. The impulse width amounts to $\Delta t = | T_1 - \tau_1 |$.

The impulse width corresponds to the delay time of the transversal wave running from plucking point to pickup. If this distance is e.g. 4 cm, the impulse width calculates as $4 \cdot T/2 \cdot 64 = T/32$. Herein, the scale is assumed to be 64 cm. If the string is plucked exactly over the pickup, the two square impulses are perfectly contiguous.

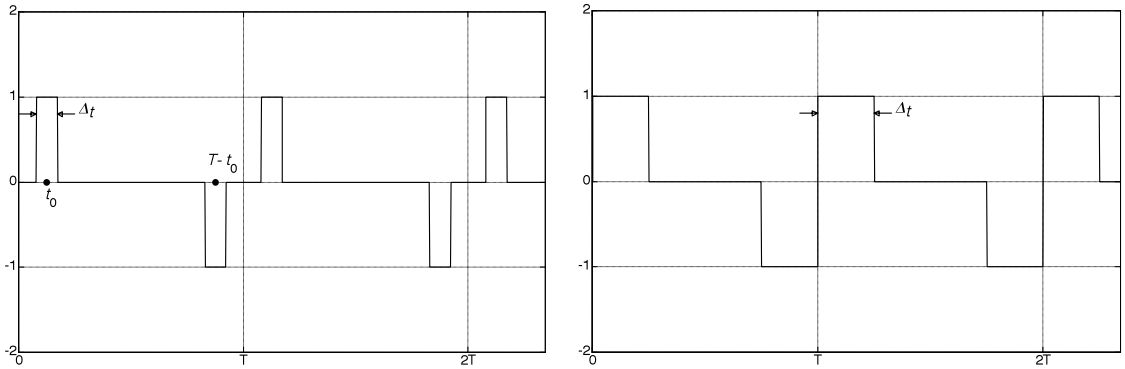

Fig. 2.31: Step response of the filter from Fig. 2.30. Left: $T_1 \neq \tau_1$; right $T_1 = \tau_1$. Input quantity for the filter is a force step at the plucking point. Output quantity is the string velocity over the magnet of the pickup – the source voltage of the pickup is proportional to this velocity. The terminal voltage results from low-pass filtering of the source voltage (Chapter 5.9). In particular for the low strings, the frequency-dependent propagation velocity (dispersion, Chapter 2.8.4) takes care of reshaping the rectangular waveform. In order to model this effect, the delays in Fig. 2.30 need to be realized as all-passes (Fig. 2.39).

The calculation of the **overall transfer function** of the 4 serially connected individual filters requires a multiplication of the individual transfer functions, resulting in somewhat more complicated frequency responses (**Fig. 2.32**).

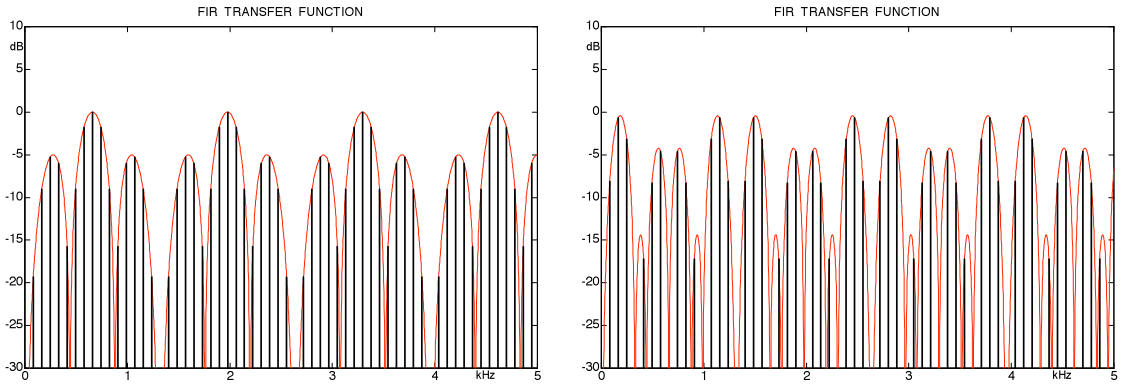

Fig. 2.32a: Transfer frequency response, E_2-string plucked 12 cm away from the bridge. Scale = 64 cm. Left: bridge-pickup (4 cm distance from the bridge); right: neck-pickup (16 cm distance from the bridge).

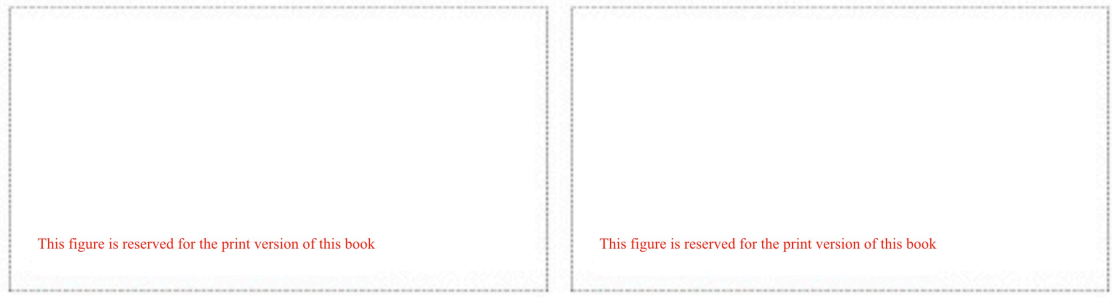

Fig. 2.32b: Transfer frequency response, string plucked 12 cm away from the bridge; bridge pickup (5cm distance from the bridge, scale = 64 cm). Left: E_2-string, right: A-string.

It should be noted as particularly important that the two FIR-filters act **string-specifically** and do not have a global filter effect (as the magnetic pickup discussed in Chapter 5 would show it). The winding of the pickup coil is permeated by field-alterations of all 6 strings, and thus the resonance peak of the pickup will affect all 6 strings in the same way. The cancellations of the FIR-filter, however, are based on the propagation speeds of the waves, and these are string specific. As already elaborated, these propagation speeds do not depend on the (fretted) pitch, but on the pitch of the open string. The latter determines the propagation speed c_P, after all. It is therefore not possible to generate the FIR-characteristic electronically with an effects device … not with your regular pickups, anyway.

Fig. 2.33 shops the FIR frequency responses of a **Stratocaster** dependent on the pickup position. The effect of the second FIR-filter (plucking location) was not included in the calculations. To ensure a clear representation, the minima are only shown to a depth of 18 dB; according to the theory, the graph should extend to $-\infty$ dB in the minima.

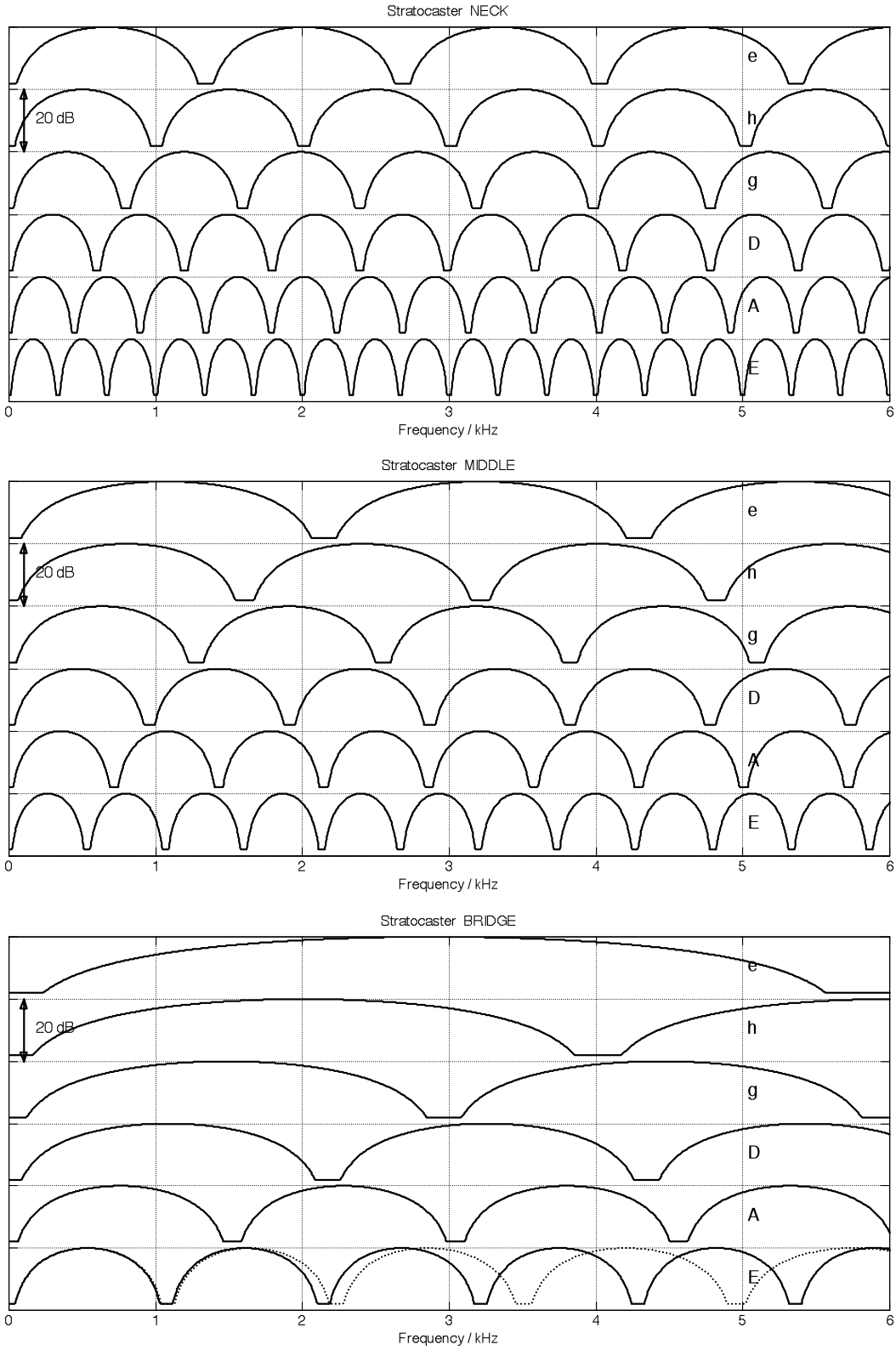

Fig. 2.33: Calculated FIR frequency responses for the Stratocaster; without dispersion. The dynamic is limited to 18 dB. In the lowermost graph, the effect of dispersive propagation is shown as a dotted line (compare to Chapter 1.8.4).

In **Fig. 2.34**, we see a comparison between measurement and calculation. A Stratocaster is connected to an instrumentation amplifier (input impedance: 100 kΩ) via a cable of a capacitance of 200 pF. The E_2-string is plucked directly at the bridge with a plectrum, and the signal of the bridge-pickup was evaluated.

The comparative calculation of the line spectrum includes both FIR-filters, the IIR-filter, and the equivalent circuit diagram of the pickup (Chapter 5.9.3). In addition, a small treble-attenuation was included to emulate the window of the magnetic field (Chapter 5.4.4). There is a clear correspondence. The measured spectrum nicely depicts the spreading of the frequency of the partials; it was emulated for the calculation using a simple model. The simulation easily reproduces the comb-filter structure, as well – at high frequencies, however, differences between measurement and calculation become evident. For a further improvement, e.g. the reflection coefficients would have to be adapted.

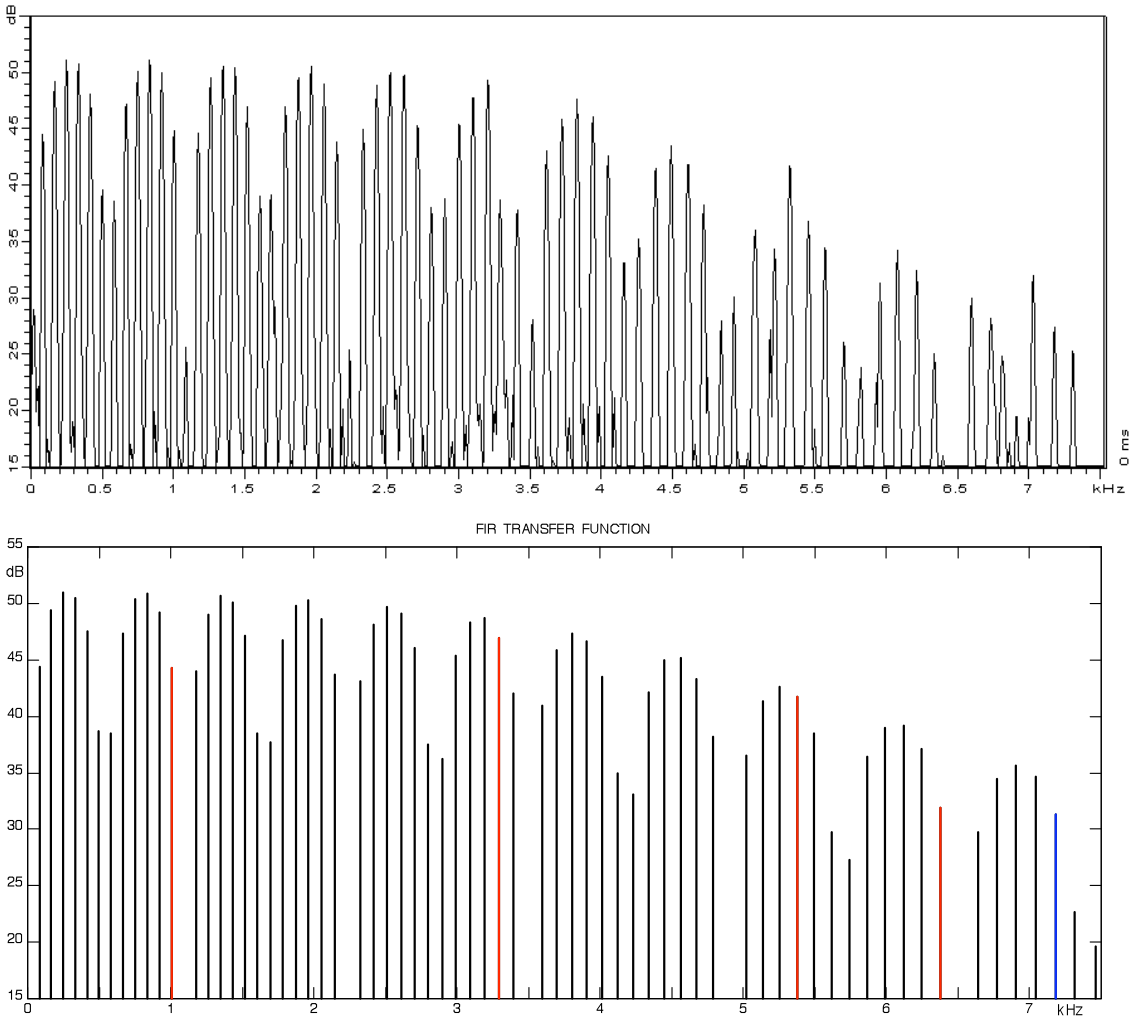

Fig. 2.34: Spectrum of an E_2-string plucked directly at the bridge (Stratocaster, middle pickup).
Top: measurement (with DFT-leakage). Bottom: calculation (with dispersion, compare to Chapter 2.8.4).
The inharmonic spreading is considerable; the 70th "harmonic" is at 7,37 kHz rather than at 5,84 kHz.

It was already noted with respect to Fig. 2.30 that the plucking point on the string and the location of the pickup result in an FIR-filter each (with different delay times). Two serially connected filters represent two *commutatively* connected mappings the sequence of which may be interchanged. It therefore should not make any difference whether the string is plucked at point A with the pickup being located at point B, or the string is plucked at point B with the pickup located at point A.

To check this hypothesis, the E_2-string of a Stratocaster was plucked over the neck-pickup while the signal from the bridge-pickup was recorded. Subsequently, the E_2-string was plucked over the bridge-pickup and the signal of the neck-pickup was recorded. **Fig. 2.35** shows the DFT-spectra of both signals. The agreement is uncanny – especially considering that the reproducibility of the plucking process is not particularly good.

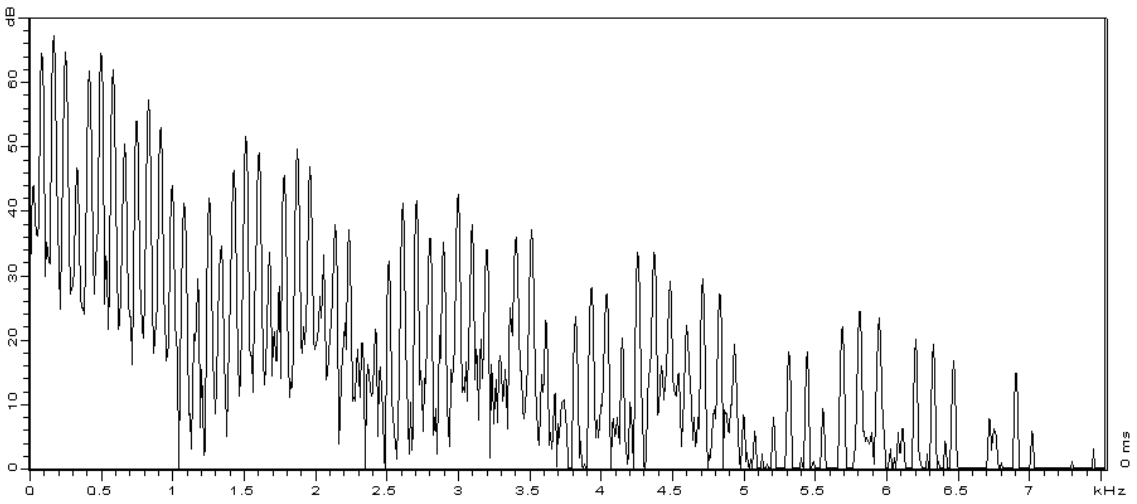

Measured signal of the bridge-pickup; string plucked over the neck-pickup.

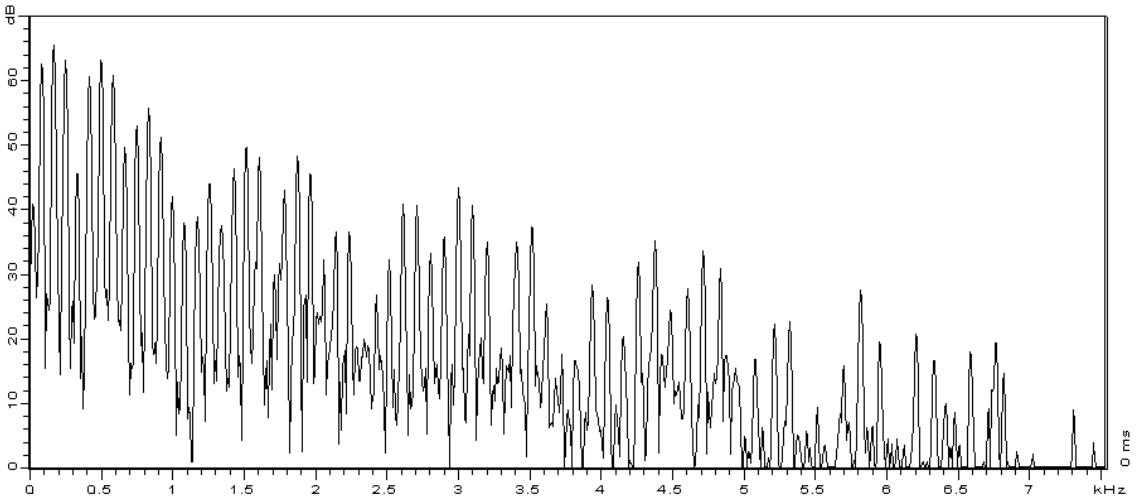

Measured signal of the neck-pickup; string plucked over the bridge-pickup.

Fig. 2.35: Spectrum of the E_2-string of a Stratocaster; pickup and plucking position interchanged.

2.8.3 String with humbucking pickup

In the hum-cancelling humbucking pickup, two coils are connected in opposite phase. In order for the electrical output signals to interact constructively, the magnetic permanent flux is reversed in one of the coils. Many pickups (e.g. Gibson) generate the permanent field using a bar magnet located under the coils; the field is conducted through the coils using so-called pole-pieces. Other designs (e.g. Fender) use 6 individual magnets in each coil; in one of the coils, the north-pole is directed upwards, in the other it is the south-pole. The two coils are usually connected serially in opposite phase; opposite-phase parallel connection is less common.

The humbucker samples a wave running along the string at two adjacent areas. The distance between the two pole-pieces is 18 mm for the Gibson Humbucker – there are, however, also very narrow humbuckers that fit into the housing of a regular single-coil pickup.

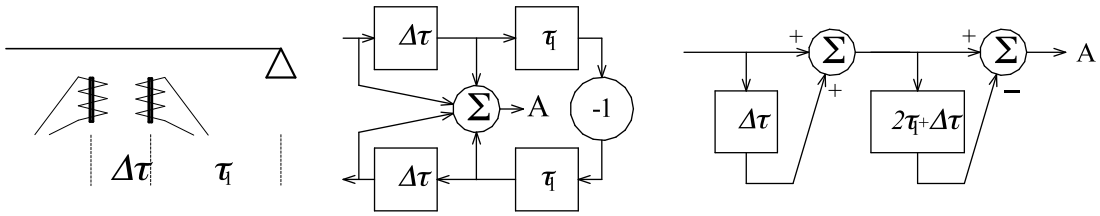

$$\underline{H}(j\omega) = 1 + e^{-j\omega\Delta\tau} - e^{-j\omega(\Delta\tau+2\tau_1)} - e^{-j2\omega(\Delta\tau+\tau_1)} = \left(1 + e^{-j\omega\Delta\tau}\right) \cdot \left(1 - e^{-j\omega(2\tau_1+\Delta\tau)}\right)$$

Fig. 2.36: Signal flow diagram for a humbucking pickup with two equivalent coils.

In **Fig. 2.36**, τ_1 represents the (single) delay time between the coil located closer to the bridge and the bridge, while $\Delta\tau$ is the delay between the two coils. Using suitable conversion, we arrive at a simple ladder-network of two FIR-filters. The first filter models – with same-phase superposition – the delay time $\Delta\tau$ between the coils; the other filter emulates – using opposite-phase superposition – double the delay time between the middle of the humbucker and the bridge. The humbucker positioned at a location x differs from a single-coil pickup located at the same position only in the $\Delta\tau$-filter. The modeling as ladder network offers the considerable advantage that the overall transfer function can be represented as the product of the individual transfer functions. Given a humbucker with a distance between pole-pieces of 18 mm, we get an additional **signal cancellation** for the E_2-string in the range around 3 kHz; for the higher strings, the humbucker-minimum is located at correspondingly higher frequencies. The exact frequency of the minimum depends not only on the pole-piece distance, but also on the dispersion (Chapter 1.3)

As is shown in **Fig. 2.37**, the differences between single-coil pickup and humbucker are string-specific: for the E_4-string, only small variations in the treble range will be recognizable, while for the E_2-string, the humbucker will absorb the 3-kHz-range that is important to obtain a brilliant sound. Reducing the distance of the two humbucker coils to 13 mm (as it was done e.g. in the **Mini-Humbucker** fitted to the Les Paul Deluxe) will shift all interference-minima toward higher frequencies. A particularly small distance of the coils (7 – 9 mm) is realized in the single-coil format; still, a treble loss remains for the low strings.

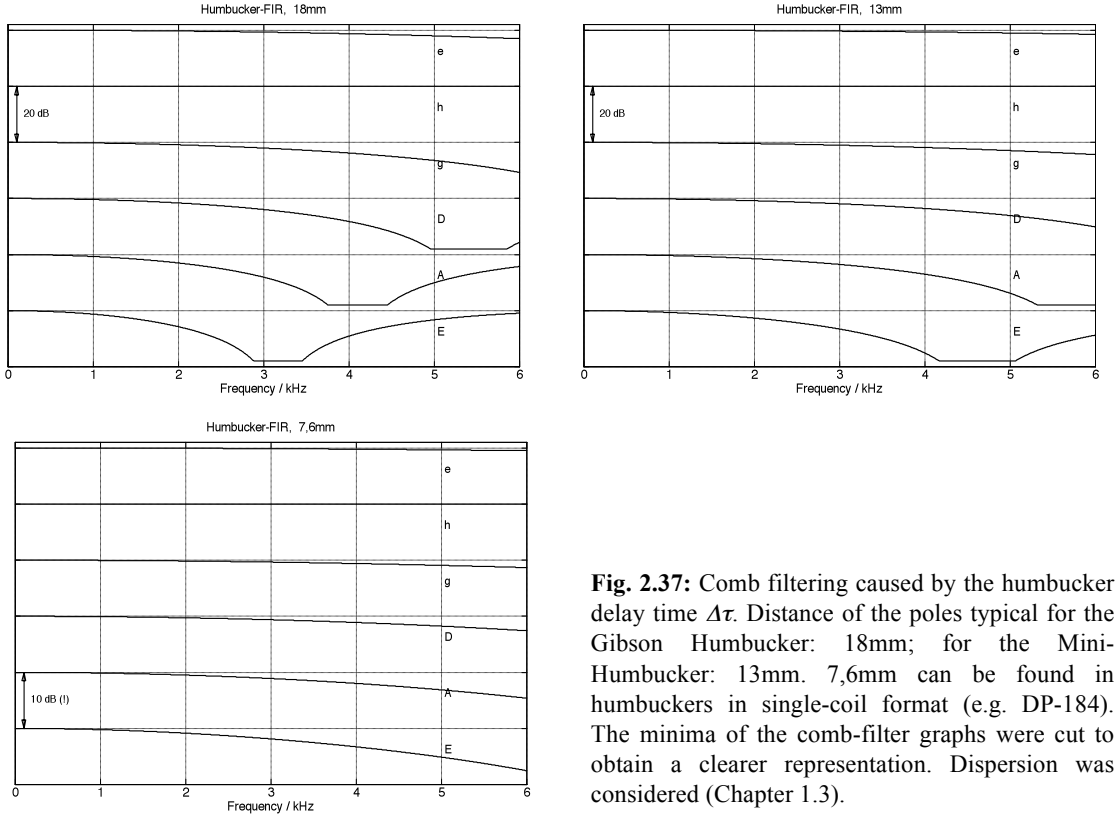

Fig. 2.37: Comb filtering caused by the humbucker delay time $\Delta\tau$. Distance of the poles typical for the Gibson Humbucker: 18mm; for the Mini-Humbucker: 13mm. 7,6mm can be found in humbuckers in single-coil format (e.g. DP-184). The minima of the comb-filter graphs were cut to obtain a clearer representation. Dispersion was considered (Chapter 1.3).

If the two humbucker coils do not feature the same sensitivity in both coils, we get differences in particular in the range of the humbucker-minimum (**Fig. 2.38**). Such **imbalances** have their roots in different numbers of the turns of the coils (deliberately produced for the *Burstbucker*) and/or in the field guides: the pole pieces in the shape of slugs have a different magnetic resistance compared to the threaded pole-screws. For differing coils, the SFD may not be separated into two FIR-filters, and thus Fig. 2.38 shows the frequency responses of the overall signal flow diagram.

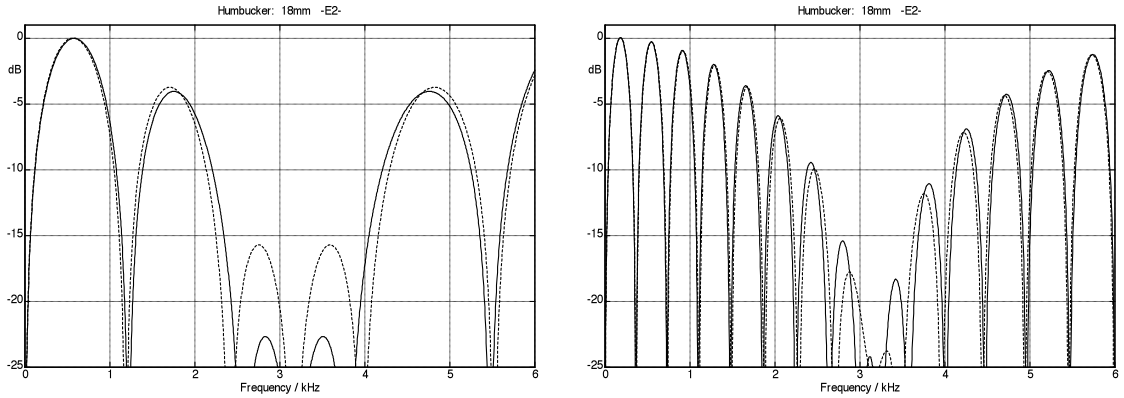

Fig. 2.38: Magnitude frequency responses for unmatched humbucker coils. Left: bridge humbucker (distance to bridge 45 mm); right: neck humbucker (distance to bridge 147 mm). The sensitivity of the coil with threaded pole pieces (screws) is better by 1 dB compared to the "slug"-coil (——), or smaller by 1 dB (---). Dispersion was considered (Chapter 1.3).

For a Gibson ES-335 TD (E_2-string), **Fig. 2.39** considers the transfer function of the equivalent circuit established in Fig. 2.36. In **Fig. 2.40**, the RLC-transfer-function (Chapter 5-9) is added in. Via **Fig. 2.41**, we can compare a measurement. For all graphs, dispersive wave propagation was included.

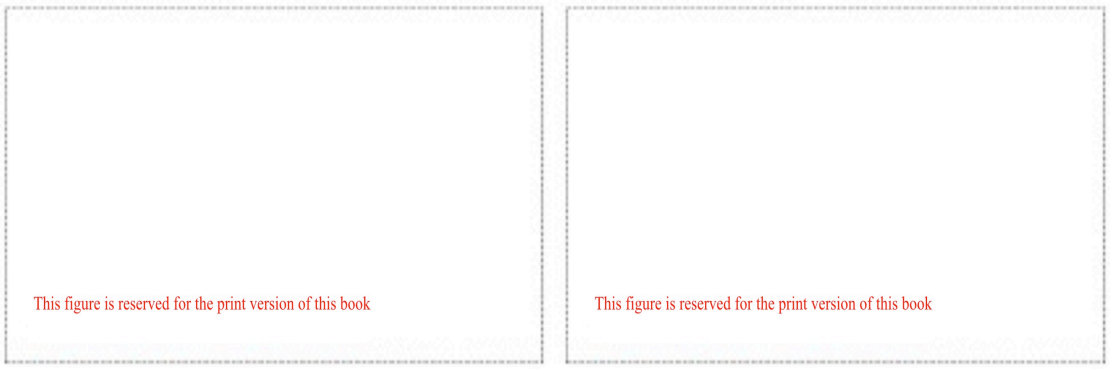

Fig. 2.39: Gibson ES335, E_2-string, model without RLC-filter. Left: bridge pickup. Right: neck pickup.

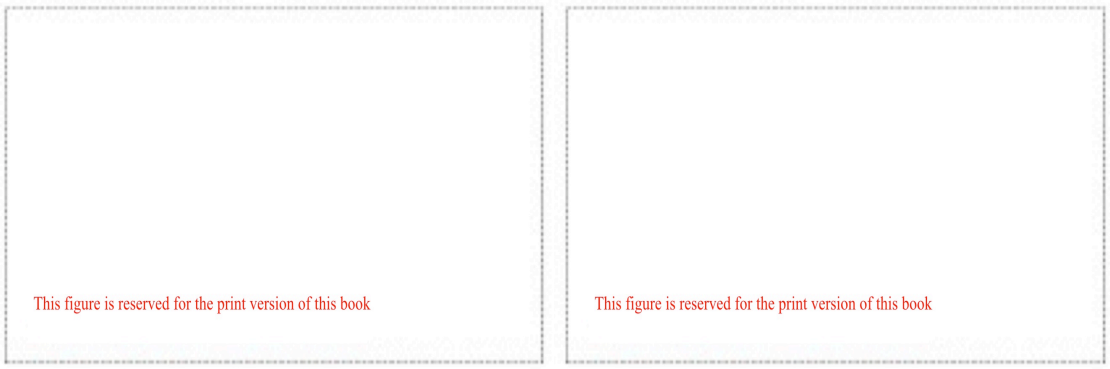

Fig. 2.40: ES335, E_2-string, model with RLC-filter and 707-pF-cable. Left: bridge pickup. Right: neck pickup.

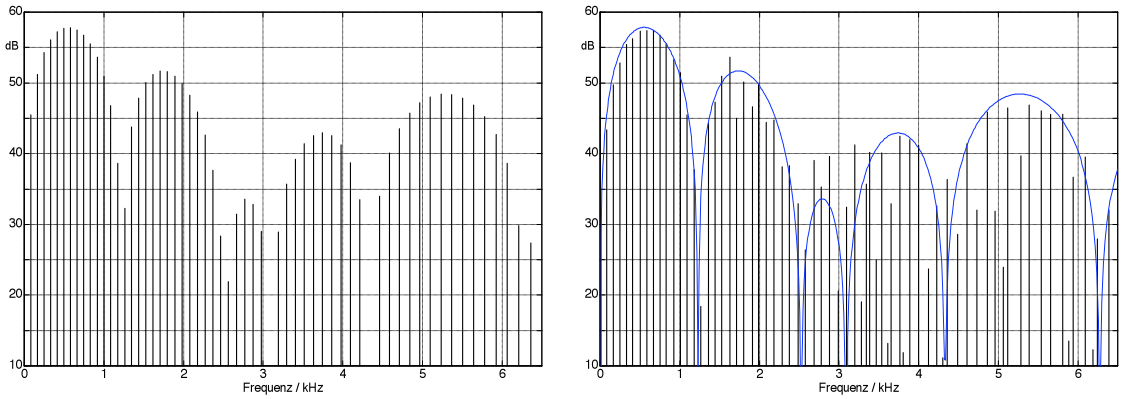

Fig. 2.41: ES335, E_2-string plucked directly at the bridge; bridge pickup. Left: model calculation; right: measurement. The differences do not refute the basic model assumptions; rather, they indicate how important the modeling of both strain-wave and bearing impedances is – this was not included here.

2.8.4 Dispersive line elements

In Chapter 1.2, we had discussed that the propagation speed of the transversal waves is frequency dependent (**dispersion**), leading to a "spreading out" of the frequencies of the partials. This effect may be modeled in the SFD using frequency-dependent delay times. If we first assume the string to be loss-free, the magnitude spectrum will not change during the wave propagation. The phase spectrum does change – but not with a linear-phase characteristic like it would in a delay line. Rather, it assumes the characteristic of an **all-pass function** due to the frequency-dependent delay time. From the spreading of the partials, we can deduce the all-pass transfer-function (Chapter 1.3.1), and from this the all-pass impulse response (Chapter 1.3.2) via inverse Fourier transform. The simulations shown in Chapter 1 were calculated using such an SFD.

All-pass: linear system with a frequency-independent magnitude transmission coefficient and frequency-dependent phase shift.
Minimal-phase system: linear all-pass-free system.
Linear-phase system: linear system with frequency-proportional phase shift.
System order: number of the independent storage elements in the system.

For a wound E_2-string (b = 1/8000), **Fig. 2.42** shows the phase shift φ as it appears in a transversal wave running the distance of 8,65 mm (Chapter 1.3.1). Cascading 74 of the digital filters indicated in the figure yields a good approximation of the overall phase-shift of an E_2-string of 64 cm length (single travel path). The relatively high number of filters is due to the chosen sample frequency: a 2nd-order all-pass can turn shift the phase by no more than 2π.

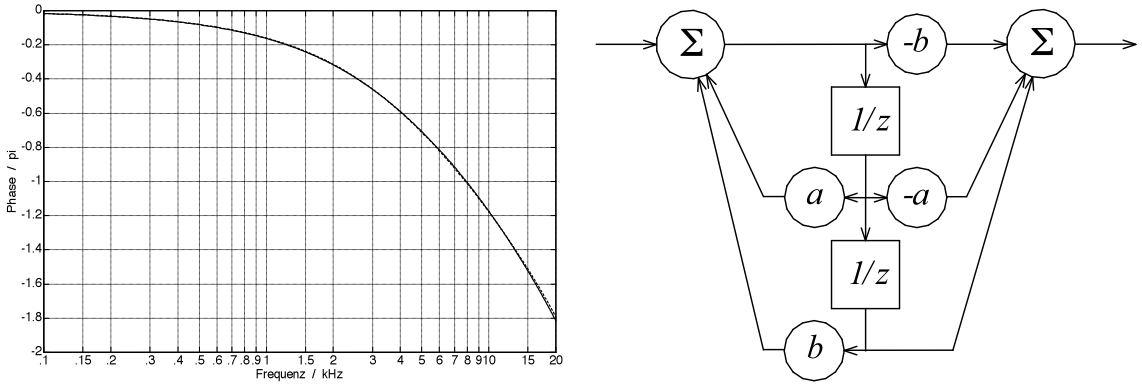

Fig. 2.42: Block-diagram and frequency response of the phase of a 2nd-oder canonic digital all-pass filter. Sample frequency: f_a = 48 kHz, a = 0,5378, b = -0,03668. The frequency response of the filter phase is indicated as a dashed line; the differences to the phase of the string (——) are insignificant. "Frequenz" = frequency.

Given f_a = sample frequency, the transfer function of the digital all-pass is:

$$\underline{H}(z) = \frac{1 - az - bz^2}{z^2 - az - b}; \qquad \left|\underline{H}(z)\right| = 1; \qquad z = \exp(j\omega / f_a)$$

If the sample frequency is changed, the parameters a and b need to be adapted, as well.

The phase delay of the all-pass filter shown in Fig. 2.42 features the same tendency as it is found in dispersive waves on strings: high frequencies get to the output of the filter faster than low ones. Given a step excitation, we will therefore see a reaction in the high frequency range first; the low frequency components follow with a delay (**Fig. 2.43**).

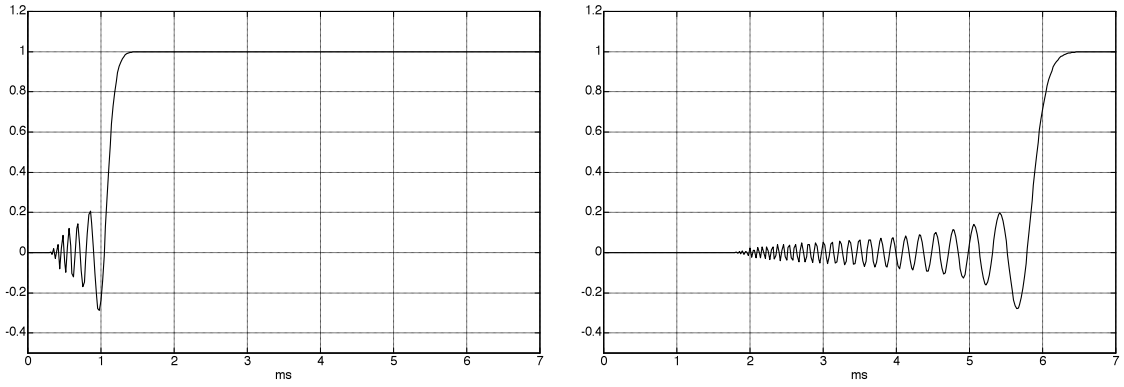

Fig. 2.43: Step response of a cascade of 14 (left) and 74 (right) all-pass filters. Data as in Fig. 2.42. In addition to the all-passes, a slight treble attenuation was included (*one* 1st-order low-pass at 10 kHz).

On the one hand, **dispersion** has the effect of a progressive spreading of the frequency of the partials. For the perceived sound, it is more important, though, that the FIR-filters depicted in Figs. 2.30 and 2.36 are subject to the same mechanism, as well: their interference effect happens progressively spread out towards higher frequencies. Given a dispersion-free E_2-string, the bridge pickup of a Stratocaster would feature an interference cancellation at $3 \cdot f_G \cdot$ 65cm / 5cm = 3214 Hz. However, your commercially available string is not free of dispersion, and therefore the interference cancellation mentioned above will happen somewhere in the range of 3330 – 3520 Hz, depending on the specific design of the string. In case the loudspeaker contributes narrow-band resonances in that same frequency range, a change of the make of strings may indeed bring audible differences. In this context, it should not be left unmentioned, though, that moving the guitar loudspeaker may well lead to changes in the sound: the room represents an FIR-filter, as well – due to the various occurring sound paths.

